ASSESSMENT OF ACCRUED THERMO-MECHANICAL DAMAGE IN LEADFREE PARTS DURING FIELD-EXPOSURE TO MULTIPLE ENVIRONMENTS

Pradeep Lall, Ph.D., Rahul Vaidya and Vikrant More
Auburn University
Department of Mechanical Engineering
and NSF Center for Advanced Vehicle and Extreme Environment Electronics (CAVE^3)
Auburn, AL, USA

Kai Goebel, Ph.D.
NASA Ames Research Center
Moffett Field, CA, USA

ABSTRACT

Electronic assemblies deployed in harsh environments may be subjected to multiple thermal environments during the use-life of the equipment. Often the equipment may not have any macro-indicators of damage such as cracks or delamination. Quantification of thermal environments during use-life is often not feasible because of the data-capture and storage requirements, and the overhead on core-system functionality. There is need for tools and techniques to quantify damage in deployed systems in absence of macro-indicators of damage without knowledge of prior stress history. The presented PHM framework is targeted towards high reliability applications such as avionic and space systems. In this paper, Sn3.0Ag0.5Cu alloy packages have been subjected to multiple thermal cycling environments including -55 to 125C and 0 to 100C. Assemblies investigated include area-array packages soldered on FR4 printed circuit cards. The methodology involves the use of condition monitoring devices, for gathering data on damage pre-cursors at periodic intervals. Damage-state interrogation technique has been developed based on the Levenberg-Marquardt Algorithm in conjunction with the microstructural damage evolution proxies. The presented technique is applicable to electronic assemblies which have been deployed on one thermal environment, then withdrawn from service and targeted for redeployment in a different thermal environment. Test cases have been presented to demonstrate the viability of the technique for assessment of prior damage, operational readiness and residual life for assemblies exposed to multiple thermo-mechanical environments. Prognosticated prior damage and the residual life show good correlation with experimental data, demonstrating the validity of the presented technique for multiple thermo-mechanical environments.

Key Words: Leadfree Alloys, Ball grid array, prognostics, solder joint fatigue, thermo-mechanical reliability

INTRODUCTION

Airborne and space electronic systems require ultra-high reliability since the cost of failure in terms of potential risk to human life is unacceptable. Avionic systems fulfill critical roles in autonomous aircraft control and navigation, flight path prediction and tracking, and self-separation. Complex electrical power systems (EPS) which broadly comprise of energy generation, energy storage, power distribution, and power management, have a major impact on the operational availability, and reliability of avionic systems. Airborne electronic systems may be deployed for very long use-life in operation. Examples include the B-52, which lifted off April 15, 1952, for a test flight. It is scheduled to fly until 2040. That would make it the longest-serving military jet in history [USA Today, April 23, 2002]. Current health management techniques in EPS and Avionic Systems provide very-limited or no-visibility into health of power electronics, and packaging to predict impending failures. [McCann 2005, Marko 1996, Schauz 1996, Shiroishi 1997]. Health monitoring systems have the potential to enhance the safe-use service life of long-life systems without compromising operational readiness.

Deployed electronic systems often may be subjected to multiple thermal environments. Thermal environments may change due to operational environments or change in usage profiles. Decision-support for re-deployment requires system data on the operational readiness of electronic systems based on accrued damage and residual life in intended environment. Current state of art relies on diagnostic detection of failure based on the built-in self test, which provides ability for error detection and correction circuits used to give electronic assemblies the ability to test and diagnose themselves with minimal interaction from external test equipment [Chandramouli 1996, Drees 2004, Hassan 1992, Williams 1983, Zorian 1994]. However, the current form of BIST provides little insight about the system level reliability or the remaining useful life of the system. Several studies conducted [Allen 2003, Drees 2004, Gao 2002, Rosenthal 1990] have shown that BIST can be prone to false alarms and can result in unnecessary costly replacement, re-qualification, delayed shipping, and loss of system availability. Fuses and Canaries may be mounted on a part to provide advance warning of failure due to specific wear out failure mechanism. Advanced

warning is used to provide a maintenance-window for correction action, after an initial failure or malfunction, to prevent additional or secondary failures [Anderson 2004]. State of art error detection and correction techniques lack the capability for assessment of prior damage and provide limited insight into estimation of remaining useful life. Future improvements in reduction of system downtime require emphasis on early detection of degradation mechanisms [Jarell 2002].

Lall, et. al. [2004[a-d], 2005[a-b], 2006[a-f], 2007[a-e], 2008[a-f]] have developed leading indicators of failure for prognostication of electronic systems under thermo-mechanical, shock-impact and vibration stresses. Proxies such as phase growth rate in solder interconnects have been identified as leading indicators of failure. The authors have previously presented a methodology for interrogation of system-damage state for single thermal cycling and isothermal aging environments [Lall 2007[c], 2008[c,d]]. In this paper, the PHM approach has been developed for interrogation of damage state for electronic systems subjected to multiple thermal environments. The approach enables assessment of accrued damage and the residual life assessment in the intended environment. The presented methodology is different from the state-of-art diagnostics and resides in the pre-failure-space of the electronic-system, in which no macro-indicators such as cracks or delamination exist. The methodology eliminates the need to capture the prior stress history for prognostication of system state. Relationships for computation of residual life have been developed based on damage proxies.

TEST VEHICLE

In the present study, ball grid area-array packages with Sn3Ag0.5Cu alloy solder interconnects assembled on FR4 laminates and ENIG board finish have been studied. The assemblies have been subjected to dual thermo-mechanical loads. Two packages studied include the 256 I/O, 17x17 mm, 1 mm pitch plastic ball grid array and the 100 I/O, 12 x 12 mm, 0.8 mm pitch packages (Figure 1). The package to chip ratio is nearly 2.14 for both packages. The chip size is 7.94 x 7.94 mm for the 256 I/O package and 5.58 x 5.58 mm for the 100 I/O package (Table 1).

The assemblies have been subjected to relatively harsh thermal cycle (TC-1) temperature ranging from -55°C to 125°C, 2.5 hours/cycle followed by a milder thermal cycle (TC-2) temperature from 0°C to 100°C, 16 minutes Dwell and 8 minutes ramp. Data on micro-structural evolution of damage has been collected by withdrawing samples periodically. Figure 2 shows the printed circuit board assembly which have been used for this experiment; all boards were No-Core assembly with Non Solder Mask Defined (NSMD) pads. The printed circuit board contains six trace layers to simulate the thermal mass of a true production board, though all functional traces have been run on the topmost layer. All the assemblies were daisy-chained and continuously monitored for failure detection during cycling.

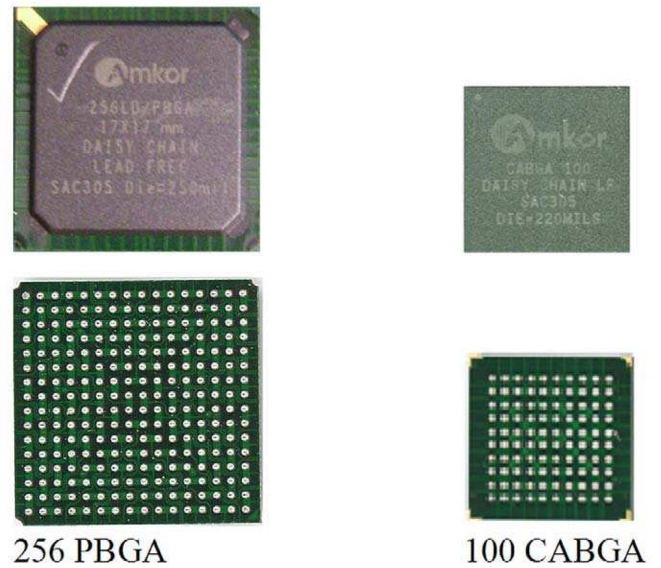

Figure 1: Test Vehicle 256 PBGA and 100 CABGA.

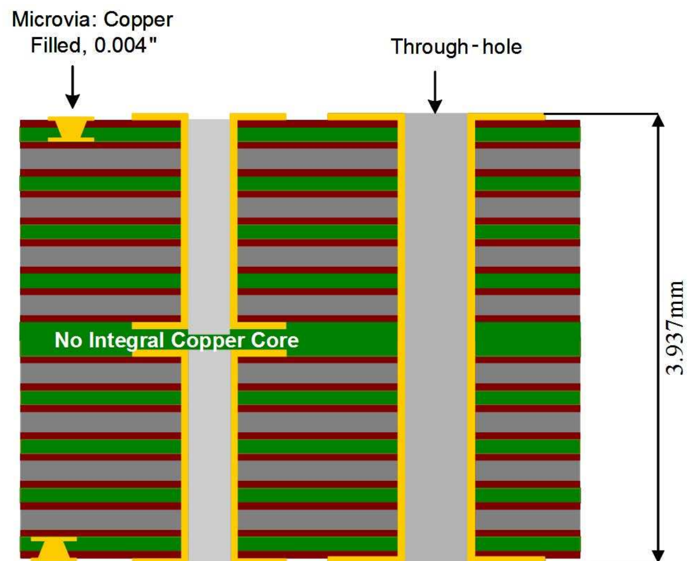

Figure 2: Printed Circuit Board Assembly Construction in the Test Assemblies.

Solder	Sn3Ag0.5Cu	Sn3Ag0.5Cu
Package Size (mm)	17 x 17	12 x 12
Package Type	PBGA	CABGA
I/O Count	256	100
I/O Pitch (mm)	1	0.8
Ball Diameter (mm)	0.5	0.5
Die Size (mm)	7.94	5.58
P/D ratio	2.14	2.15
Board Finish	ENIG	ENIG
Substrate Pad Type	NSMD	NSMD

Table 1: Package Architecture Details for Test Vehicle.

PROGNOSTICATING DAMAGE IN MULTIPLE THERMO-MECHANICAL ENVIRONMENTS

The test vehicle was subjected to two-sequential thermal environments. First environment (TC-1) is a -55°C to 125°C thermal cycle, 2.5 hours per cycle and the second environment is a 0°C to 100°C thermal cycle with 16 minutes dwell time and 8 minutes ramp time. Previously, it has been shown that the rate of change in phase growth parameter [d(lnS)/d(lnN)] is valid damage proxy for prognostication of thermo-mechanical damage in solder interconnects and assessment of residual life [Lall 2004[a], 2005[a], 2006[c,d], 2007[c,e], 2008[c,d]]. The damage proxy [d(lnS)/d(lnN)] is related to the microstructural evolution of damage by the following equation:

$$S = g^4 - g_0^4 = a(N)^b \quad (1)$$

$$\ln S = \ln(g^4 - g_0^4) = \ln a + b \ln N$$

$$\frac{d(\ln S)}{d(\ln N)} = b \quad (2)$$

Where, g is the average grain size at time of prognostication, g_0 is the average grain size of solder after reflow, N is the number of thermal cycles, S is the phase growth parameter, parameters a and b are the coefficient and exponent respectively. The log-plot of the equation provides a straight line relationship between the phase growth parameter and the number of cycles. It is anticipated that the higher temperature cycle magnitude will result in more accrued thermo-mechanical damage and a higher slope of the phase growth parameter versus number of thermal cycle curve. A combined plot for TC-1 and TC-2 in terms of damage accrual proxy and life in terms of number of cycles is shown in Figure 3. TC-2 has a smaller temperature range compared with TC-1 and thus a lower slope of accrued damage proxy versus cyclic life plot. A schematic of the anticipated accrued damage versus cyclic life plots are shown in Figure 3.

Temperature excursions during operation of a circuit are due to both power-cycling and variations in ambient conditions resulting in thermo-mechanical cyclic stresses and strains induced primarily by thermal expansion mismatch between the package and the board assembly. Previous researchers have studied the micro structural evolution of ternary SnAgCu alloys at elevated temperatures using bulk real solder joints with different designs, geometry and process conditions. The SnAgCu microstructure comprises Ag_3Sn and Cu_6Sn_5 dispersed within the tin matrix. The relatively low percentage of alloying elements, 1-4% for Ag and 0.5% for Cu results in phases which comprise a small percentage of the total volume within the solder joint. The microstructural evolution of SnAgCu alloys over time has been found to effect the thermo-mechanical properties and damage behavior [Ye 2000, Allen 2004[a,b], Kang 2004, Xiao 2004, Henderson 2004, Kang 2005, Korhonen 2007, Jung 2001].

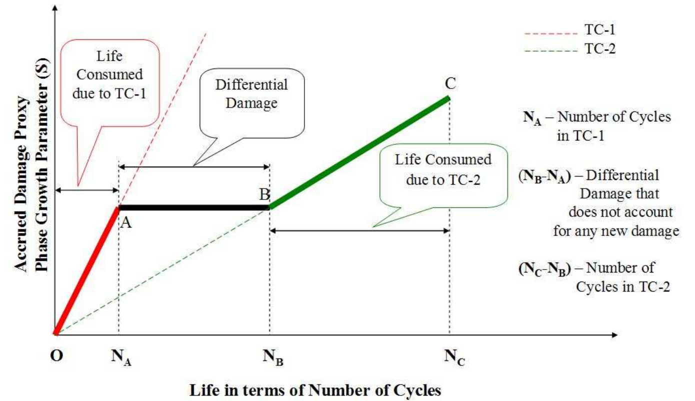

Figure 3: Life Vs Damage Curve for Multiple Thermal Environments.

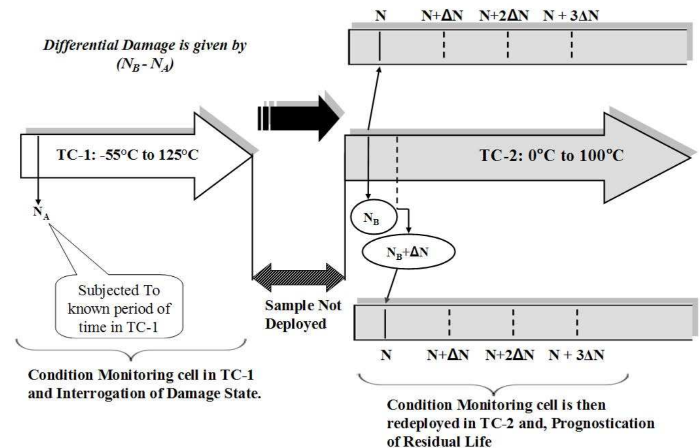

Figure 4: Problem Definition for Prognostication, Interrogation of System State and Decision Flow for Electronic Assembly Subjected to Multiple Operational Environments.

Micro-structural coarsening during thermo-mechanical deformation is attributed to the generation of excess vacancies caused by the combined effect of local hydrostatic state of stress, and the instantaneous inelastic strain rate [Dutta 2003[a], 2003[b], 2004; Jung 2001]. Evolution of solder microstructure in 63Sn37Pb and lead-free chip resistor solder joints due to thermal fatigue have been studied previously by previous researchers [Sayama, et al. 1999, 2003] and thermal fatigue correlated with occurrence of microstructural coarsening in the fatigue damaged region in of 63Sn37Pb solder interconnects [Frear 1990, Morris 1991]. Correlation of grain coarsening with thermal fatigue has also been established for high-lead solders [Bangs 1978, Wolverton 1987, Tribula 1989]. Previously the authors have investigated the grain-size evolution and derivatives of phase growth rate as prognostics parameters on a wide range of leaded and Sn4Ag0.5Cu devices in underhood applications [Lall 2004[a], 2005[a], 2006[c,d], 2007[c,e], 2008[c,d]].

The problem definition consists of an electronic assembly which has been subjected to X cycles of the field environment (TC-1) and followed by Y cycles of field environment (TC-2). In operational deployed equipment, the number of cycles may be calculated from the time in operation and the duty-cycle of the exposure in terms of number of cycles per day. The electronic assembly will thus be exposed to (X+Y) cycles of sequential application of TC-1 followed by TC-2 (Figure 4). While the field environment may consist of multiple such environments, in this paper electronic assemblies exposed to only two environments have been prognosticated in order to create a framework for multi-environment prognostication.

Prior Damage in TC-1

Consider an assembly, which has been subjected to N_A cycles in environment TC-1 with the corresponding phase growth S_A. The assembly is then withdrawn from service and assessed for operational readiness in a new environment TC-2. Assessment will include withdrawal of samples from the prognostication sensor cells and interrogation of damage state based on micro-structural evolution of damage. The prior accrued damage sustained by the system in TC-1 has been prognosticated by withdrawing 4-samples in the prognostication time neighborhood.

$$\begin{aligned} S_A &= g_A^4 - g_0^4 = a(N_A)^b \\ S_{A+\Delta N} &= g_{A+\Delta N}^4 - g_0^4 = a(N_A + \Delta N)^b \\ S_{A+2\Delta N} &= g_{A+2\Delta N}^4 - g_0^4 = a(N_A + 2\Delta N)^b \\ S_{A+3\Delta N} &= g_{A+3\Delta N}^4 - g_0^4 = a(N_A + 3\Delta N)^b \end{aligned} \quad (3)$$

The equations are solved using the LMF Algorithm. Solution is identified as the dataset with the minimum error in the solution space. In this case, prognostication yields values of g_0, a, b, N_A. In order to distinguish them from the experimentally observed values, the subscript "p" has been appended at the each of each parameter. The parameters are thus, g_{0p}, a_p, b_p, N_{Ap}. The prognosticated value of prior damage in TC-1 is denoted by N_{Ap}. The prognosticated value of sustained damage, N_{Ap}, should be in the neighborhood of the actual sustained damage N_A within the margin of error.

Operational Readiness for TC-2

In order to assess the operational readiness of the electronic assembly in TC-2, the prognostic sensor cells are subjected to a small period of exposure of TC-2. Samples from the prognostic sensor cells are then withdrawn for computation of residual life. Note that the micro-structural evolution of damage from S_0 to S_A is path independent, i.e. the phase coarsening from S_0 to S_A may be achieved in environment TC-1 in period N_A or in environment TC-2 in a period N_B (i.e., $g_A = g_B$; and $S_A = S_B$). The differential damage is computed by exposing the samples to incremental damage in the new environment TC-2. The initial phase size, g_{0p}, is expected to be identical regardless of the thermal environment, to which the assemblies have been exposed.

$$\begin{aligned} S_B &= g_B^4 - g_0^4 = a(N_B)^b \\ S_{B+\Delta N} &= g_{B+\Delta N}^4 - g_0^4 = a(N_B + \Delta N)^b \\ S_{B+2\Delta N} &= g_{B+2\Delta N}^4 - g_0^4 = a(N_B + 2\Delta N)^b \\ S_{B+3\Delta N} &= g_{B+3\Delta N}^4 - g_0^4 = a(N_B + 3\Delta N)^b \end{aligned} \quad (4)$$

Where, ΔN is finite number of cycles (e.g. 50 cycles) in thermal-cycling environment. Four samples are withdrawn in the prognostication time neighborhood. The differential damage is then computed using the equation:

$$\Delta D = N_{Bp} - N_{Ap} \quad (5)$$

The equivalent damage sustained by the assembly, in TC-2 could be derived from the prognosticated prior-damage in TC-1, using the equation:

$$N_{Bp} = N_{Ap} + \Delta D \quad (6)$$

The differential damage will be known from the micro-structural evolution of the solder interconnects for the alloy system of interest.

Assessment of Residual life in TC-2

In order to assess the residual life of the electronic-assembly in TC-2 after it has been deployed for a period of time (Point-C, Figure 3), the prognostication cells will be used to estimate accrued damage. The prior accrued damage sustained by the system in TC-1 and TC-2 has been prognosticated by withdrawing 4-samples in the prognostication time neighborhood.

$$\begin{aligned} S_C &= g_C^4 - g_0^4 = a(N_C)^b \\ S_{C+\Delta N} &= g_{C+\Delta N}^4 - g_0^4 = a(N_C + \Delta N)^b \\ S_{C+2\Delta N} &= g_{C+2\Delta N}^4 - g_0^4 = a(N_C + 2\Delta N)^b \\ S_{C+3\Delta N} &= g_{C+3\Delta N}^4 - g_0^4 = a(NC + 3\Delta N)^b \end{aligned} \quad (7)$$

Where, ΔN is finite number of cycles (e.g. 50 cycles) in thermal-cycling environment. The prior damage will be assessed using the following equation:

$$N_C - N_B = N_{CP} - \Delta D - N_{AP} \quad (8)$$

The prognostication value of prior damage N_{CP} assumes that the electronic assembly has been in the second environment TC-2 for the complete time of operation. Differential damage and the prior damage accrued in first environment have been subtracted to account for the sequential thermal exposures. The method for interrogation of system state and prognostication of damage is described in the next section.

MICRO-STRUCTURAL EVOLUTION OF DAMAGE

Samples were cross-sectioned at various level of thermal cycling. The cross-sections were studied by scanning electron microscopy (SEM) using a JEOL JSM 840 instrument operated at an accelerating voltage of 20 kV. All samples were imaged as polished. The quantitative measure of Ag_3Sn particle size was established from a 100 µm x 75 µm rectangular region selected from a backscattered SEM image of a highest strain corner solder ball. The typical SEM pictures before and after the mapping of phase size using image analysis is shown in Figure 5 and Figure 6. The average phase size, g, in the selected region is measured using Image Analysis Software. The phase growth parameter, S, can be expressed as

$$S = g^4 - g_0^{\ 4} \tag{9}$$

Where, is the average phase size of solder after reflow at zero thermal cycles. The average phase growth parameter S, changes with the time in thermal cycle environment. Most of the SnAgCu solder is comprised of Sn-phases, so that the growth rate of tin and Ag_3Sn intermetallic crystals are significant. Since Ag atoms have a higher diffusion rate in the molten solder, they can diffuse out of the way and thus allow the Sn dendrites to grow. Particles of Ag_3Sn grow either to spheres or to needles shape. Since tin cannot anticipate the shape of the Ag_3Sn intermetallic particles, they have to grow ahead of the tin phase [Stromswold, 1993].

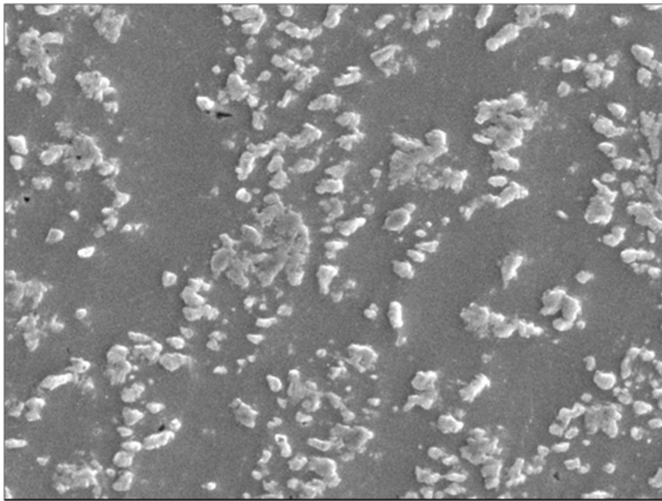

Figure 5: Micrograph from 256 I/O PBGA showing Tin and Ag_3Sn Phases.

The fundamental reason for selection of Microstructure growth and its derivatives is that, superplastic alloys are usually made of fine grain structure. Therefore a considerable growth of the matrix grains and the second phase particles frequently occur during high temperature deformation. Quantitative metrics of changes in microstructure have been identified and relationships developed to represent damage progression. The phase growth parameter has been defined as the relative change from phase-state after reflow, instead of the absolute value of phase state and is used as a damage precursor to compute residual life [Lall 2004[a], 2005[a], 2006[c,d], 2007[c,e], 2008[c,d]]. The relation between phase growth parameter and time for polycrystalline material is given by [Callister 1985].

$$g^n - g_0^{\ n} = Kt \tag{10}$$

where g is the average grain size at time t, g_0 is the average grain size of solder after reflow, K and n (varies from 2 to 5) are time independent constants. Various "n" values represent different rate-controlling mechanisms for Phase Coarsening.

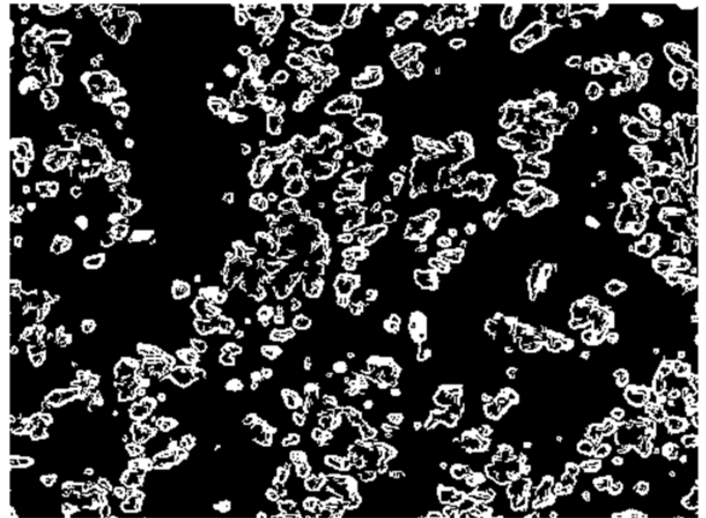

Figure 6: Microstructure Mapping using Image Analysis.

LEVENBERG-MARQUARDT ALGORITHM

The relationship between the phase growth parameter and time is nonlinear because it contains terms with fourth power. Inverse solution for interrogation of system-state is challenging for damage evolution in such systems. Levenberg-Marquardt (LM) algorithm is an iterative technique that computes the minimum of a non-linear function in multi-dimensional variable space [Madsen 2004, Lourakis 2005, Nielsen 1999]. It has been used successfully for computation of nonlinear least-square solutions. The Levenberg-Marquardt method with a combination of steepest descent using line-search and the Gauss-Newton method has been used for solution of the problem.

Let f be a assumed functional relation between a measurement vector referred to as prior-damage and the damage parameter vector, p, referred to as predictor variables. Mathematically, the function, f, which maps a parameter vector $p \in Rm$ to an estimated measurement vector is represented as, $x = f(p)$ $x \in Rn$. The measurement vector is the current values of the leading-indicator of failure and the parameter vector includes the prior system state, and accumulated damage and the damage evolution parameters. An initial parameter estimate p0 and a measured vector x are provided and it is desired to find the parameter vector p, that best satisfies the functional relation f i.e. minimizes the squared distance or squared-error, $g(p)^T g(p) = \varepsilon^T \varepsilon$ with $g(p) = \varepsilon = x - f(p)$. Assume that $\varepsilon^T \varepsilon$ is the squared error. The basis of the LM algorithm is a linear approximation to g in the neighborhood of p. For a small δp, a Taylor series expansion leads to the approximation

$$g(p + \delta p) \approx g(p) + J(p)\delta p \tag{11}$$

Where, J = Jacobian matrix $\partial g(p)/\partial p$. For each step, the value of δp that minimizes the quantity $\varepsilon = x - Jg(p)$, has been computed. Then the minimizer parameter vector, p, for the error function has been represented as,

$$F(p) = \frac{1}{2}\sum_{i=1}^{m}(g_i(p))^2 = \frac{1}{2}g(p)^T g(p) \tag{12}$$

$$F'(p) = J(p)^T g(p) \tag{13}$$

$$F''(p) = J(p)^T J(p) + \sum_{i=1}^{m} g_i(x) g_i''(x) \tag{14}$$

Where F(p) represents the objective function for the squared error term $\varepsilon^T\varepsilon$, J(p) is the Jacobian, and F'(p) is the gradient, and F"(p) is the Hessian. An initial parameter estimate p_0 and a response-vector "x" are provided and it is desired to find the vector p+, that best satisfies the functional relation x=f(p), while minimizing the squared distance $\varepsilon^T\varepsilon$. The steepest gradient descent method has been used to impose the descending condition, i.e., $F(p_{k+1})<F(p_k)$. Depending on the starting guess p0, a given function may have numerous minimizers, not necessarily the global minima. It therefore becomes necessary to explore the whole bounded space to converge to the global minima. Iteration involves finding a descent direction "h" and a step length giving a good decrease in the F-value. The variation of an F-value starting at "p" and with direction "h" is expressed as a Taylor expansion, as follows:

$$F(p + \alpha h) = F(p) + \alpha h^T F'(p) + O(\alpha^2) \tag{15}$$

Where α is the step-length from point "p" in the descent direction, "h". For a sufficiently small α, $F(p+\alpha h) \cong F(p) + \alpha h^T F'(p)$. If F(p+αh) is a decreasing function of α at α=0, then 'h' is the descent direction. Mathematically, "h" is the descent direction of F(p) if $h^T F'(p) < 0$. If no such "h" exists, then F'(p)=0, showing that in this case the function is stationary. Since the condition for the stationary value of the objective function is that the gradient is zero, i.e. f'(p+h)=L'(h)=0. The descent direction can be computed from the equation,

$$(J^T J)h_{gn} = -J^T g \tag{16}$$

In each step, Newton method uses α=1, and $p=p+\alpha h_{gn}$, where subscript 'gn' indicates gauss-newton. The value of α is found by line search principle described above. Levenberg-Marquardt algorithm is a hybrid method which utilizes both steepest descent principle as well as the Gauss-Newton method. When the current solution is far from the correct one, the algorithm behaves like a steepest descent method: slow, but guaranteed to converge. When the current solution is close to the correct solution, it becomes a Gauss-Newton method. The LM method actually solves a slight variation of Equation (16), known as the augmented normal equations.

$$(J^T J + \mu I)h = -J^T g \tag{17}$$

The term μ is called as the damping parameter, μ>0 ensures that coefficient matrix is positive definite, and this ensures that h is a descent direction. When the value of μ is very small, then the step size for LM and Gauss-Newton are identical. Algorithm has been modified to take the equations of phase growth and inter-metallic growth under both iso-thermal aging and cycling loads to calculate the unknowns.

CASE-STUDY: PROGNOSTICATION IN MULTIPLE THERMO-MECHANICAL ENVIRONMENTS

Step-1: Prognostication of Prior Damage Thermal Environment-1, TC-1

Data-Set 1a: An assembly with 100 I/O CABGA and 256 I/O PBGA packages was subjected to thermal conditions TC-1 and TC-2 for known periods of time. In this case, samples have been withdrawn after 250 cycle increments. The withdrawn samples have been cross-sectioned and the grain structure studied in an SEM. The image analysis software has been used to measure the average phase size of the Ag_3Sn and Cu_6Sn_5 phases.

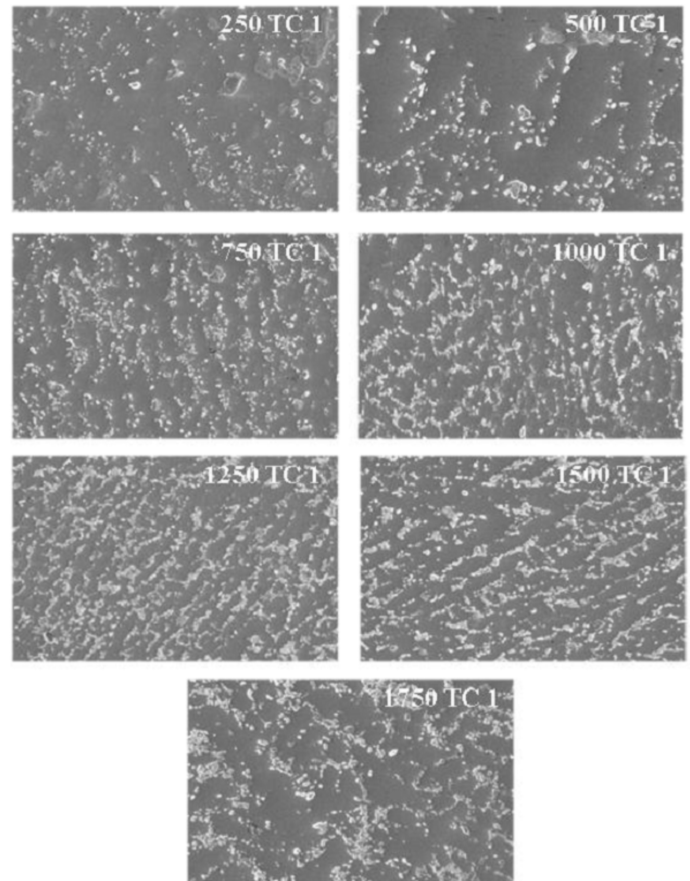

Figure 7: SEM backscattered images of phase growth versus thermal cycling (-55°C to 125°C, 96.5Sn3.0Ag0.5Cu solder, 100 I/O CABGA, magnification 750x).

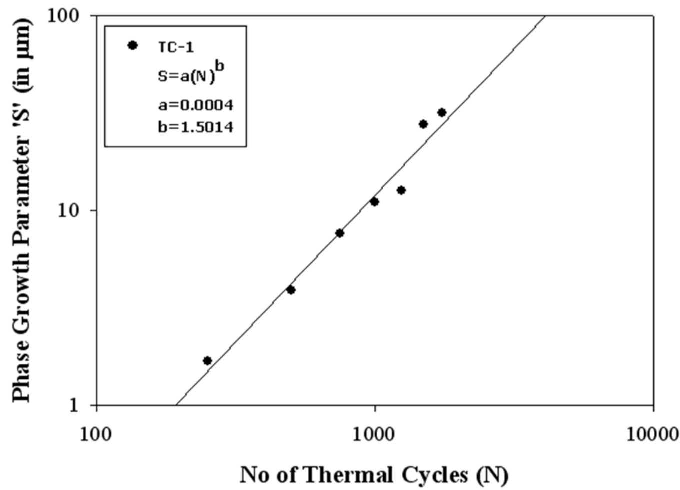

Figure 8: Phase growth Vs Number of cycles for 96.5Sn3.0Ag0.5Cu solder, 100 CABGA, subjected to TC-1 (-55°C to 125°C).

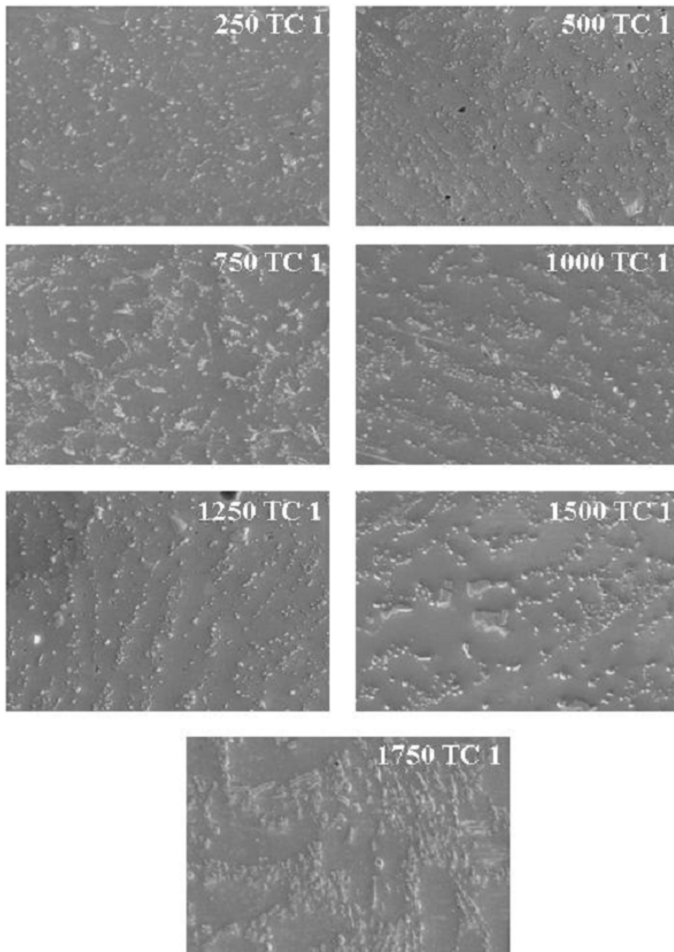

Figure 9: SEM backscattered images of phase growth versus thermal cycling (-55°C to 125°C, 96.5Sn3.0Ag0.5Cu solder, 256 I/O PBGA, magnification 750x).

Figure 7 and Figure 9 shows the phase structure of the solder at various intervals of time. Cross-sections show noticeable phase coarsening with increased thermal cycling. The plot of phase growth (S) versus number of cycles (N) in each environment is shown in Figure 8 and Figure 10. The data-set 1a will not be needed or exist in the operational assemblies. However, in the present case, the dataset has been gathered for validation of the presented approach.

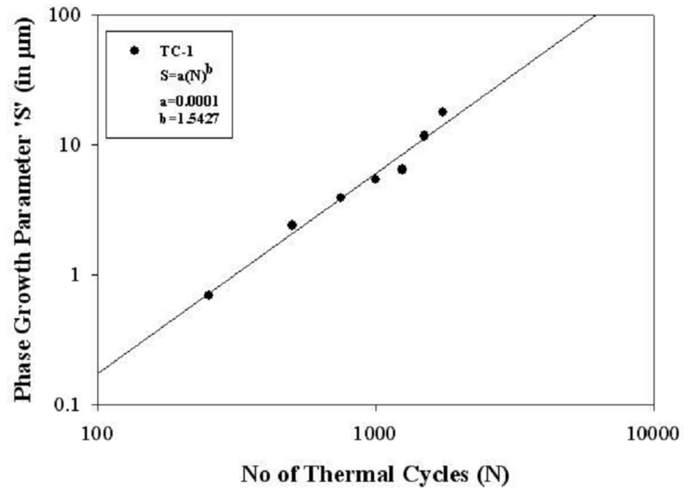

Figure 10: Phase growth Vs Number of cycles for 96.5Sn3.0Ag0.5Cu solder, 256 PBGA, subjected to TC-1 (-55°C to 125°C).

Data-Set 1b: A second set of test assemblies consisting of the 100 I/O CABGA and 256 I/O packages was subjected to thermal condition TC-1 for a known but undisclosed period of 500 cycles. This is equivalent to an electronic assembly that has been previously deployed and then withdrawn from service and assessed for prior damage. The prior damage sustained in the assemblies has been prognosticated based on micro-structural evolution of damage using measurements of phase growth. In order to prognosticate damage, the packages have been subjected to a small additional number of cycles in TC-1.

Prognostication will generally involve withdrawal of samples from condition monitoring cells towards the end of the deployment of the electronic assembly in the operating environment TC-1. In this case, samples have been withdrawn after 50 cycle increments. The withdrawn samples have been cross-sectioned and the grain structure studied in an SEM. The samples were prognosticated using the Levenberg-Marquardt Algorithm. Figure 11 and Figure 12 show the estimation of prior damage based on the LMF algorithm. The prognosticated damage at 500 cycle for the 100 I/O and 256 I/O parts is 450 cycles and 675 cycles respectively.

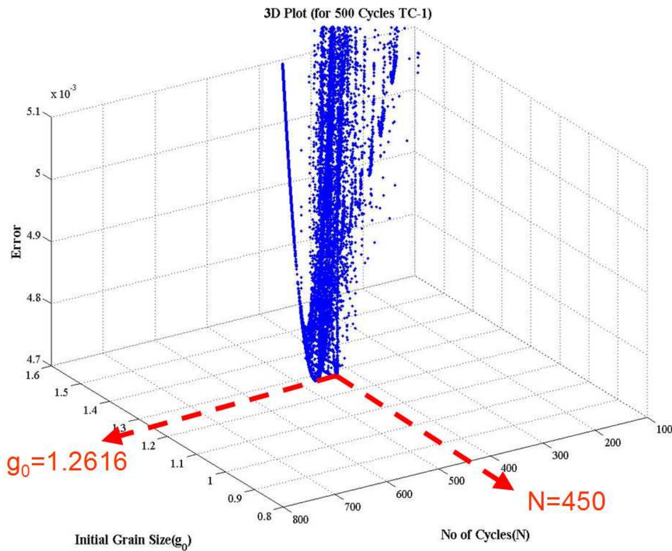

Figure 11: 3D Plot of Error Vs No of Thermal Cycles (N) for 100 CABGA 96.5Sn3.0Ag0.5Cu solder interconnects for 500 Cycles TC-1. (LM Algorithm)

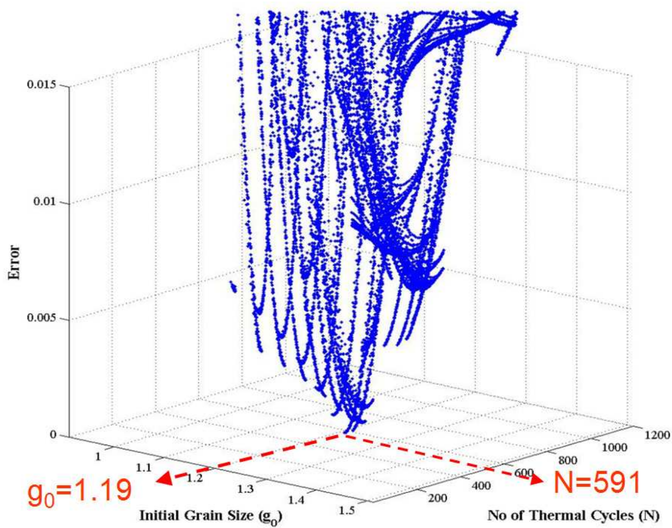

Figure 12: 3D Plot of Error Vs No of Thermal Cycles (N) for 256 PBGA 96.5Sn3.0Ag0.5Cu solder interconnects for 500 Cycles TC-1. (LM Algorithm)

Cycle Count	Cycle 'N'			Initial Grain Size 'g_0' (μm)		
	Expt Data	LM Alg	% Error	Expt Data	LM Alg	% Error
100 I/O CABGA	500	430	-14	1.258	1.076	-14.5
256 I/O BGA	500	591	18.2	1.065	1.262	18.5

Table 2: Comparison of experimental and prognosticated values of N and g_0, from for the 100 I/O CABGA, and 256 I/O PBGA with SAC305 interconnects.

Step-2: Calculation of Differential Damage (N_B-N_A) and Operational Readiness in TC-2

In this step the differential damage has been computed in electronic test-assemblies which have been exposed to 500 cycles of TC-1 (-55 to 125°C). The test assemblies would have achieved the same phase growth in a longer period of time if exposed to cycle TC-2 (0 to 100°C). A second set of assemblies was used for prognosticating operational readiness for environment TC-2. Samples from the condition monitoring cells of the electronic assemblies were exposed to a second environment TC-2 and withdrawn in the prognostication neighborhood. In this case, samples have been withdrawn after 50 cycle increments in TC-2. The withdrawn samples have been cross-sectioned and the grain structure studied in an SEM. The samples were prognosticated using the Levenberg-Marquardt Algorithm. Figure 13 and Figure 14 show the equivalence of prior damage based on the LM algorithm.

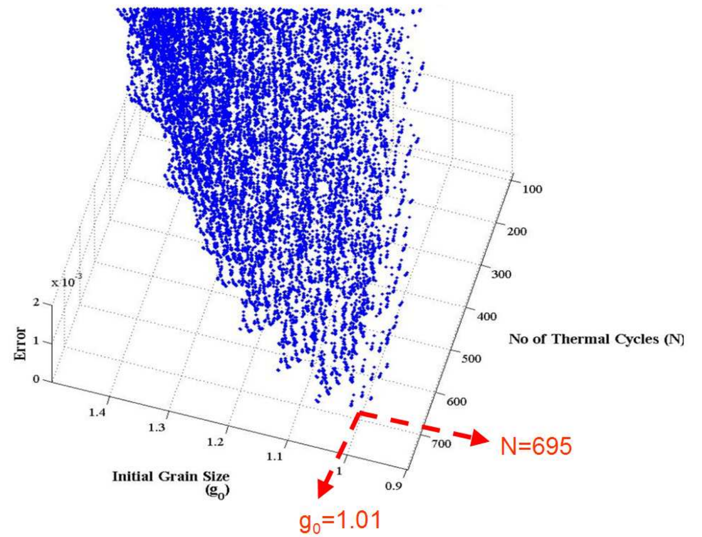

Figure 13: Differential Damage for assemblies subjected to Multiple Environments. 500 Cycles TC-1 equivalence with 662 cycles of TC-2, SAC305 solder, 100 CABGA, Magnification 750x. Prognosticated Value is 695.

It is shown that 500 Cycles TC-1 equivalences with 662 cycles of TC-2, for the 100 I/O CABGA with SAC305 interconnects. The prognosticated value is 695 cycles. In addition, 500 Cycles TC-1 equivalences with 708 cycles of TC-2, for the 256 I/O PBGA with SAC305 interconnects. Prognosticated Value is 675. Table 3 shows the comparison of the experimental and prognosticated values of differential damage between TC-1 and TC-2 for the 100 I/O CABGA and the 256 I/O PBGA. The experimental values of differential damage have been calculated based on the validation data-set by equivalency of the phase size corresponding to the multiple environments with that of the single environment. The prognosticated values of differential damage have been calculated based on the difference between the prognosticated of the packages in TC-2 and the life in TC1.

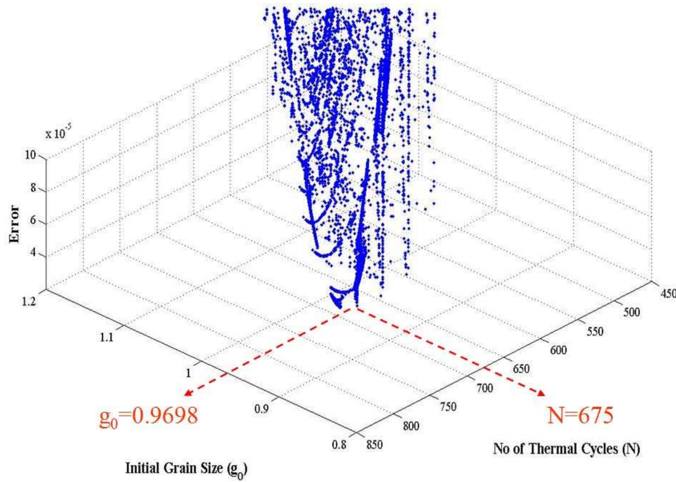

Figure 14: Differential Damage for assemblies subjected to Multiple Environments. 500 Cycles TC-1 equivalence with 708 cycles of TC-2, SAC305 solder, 256 PBGA, Magnification 750x. Prognosticated Value is 675.

Cycles		100 I/O CABGA	256 I/O PBGA
a (TC-2)		6.90E-03	1.30E-03
b (TC-2)		0.9757	1.1462
g_0		1.258	1.065
g_B		1.591	1.386
Experimental Data	Cycles of TC-1	500	500
	Cycles of TC-2	662	708
	ΔD_e (N_B - N_A)	162	208
Prognostication	Cycles of TC-2	695	675
	ΔD_p (N_B - N_A)	195	175

Table 3: Comparison of experimental and prognosticated values of differential damage for the 100 I/O CABGA, and 256 I/O PBGA with SAC305 interconnects.

Step-3: Assessment of Prior Accrued Damage and Residual life after Withdrawal from TC-1 and Redeployment in TC-2

Since the test method is destructive, the samples withdrawn for condition monitoring for Step-1 and Step-2, were discarded after the microstructural data had been gathered from the assemblies. In operational equipment, the prior damage in the withdrawn electronic assemblies will be documented and the assemblies will then be stored till such a time as deployment in a second operational environment is required. In this case, the second operational environment is TC-2.

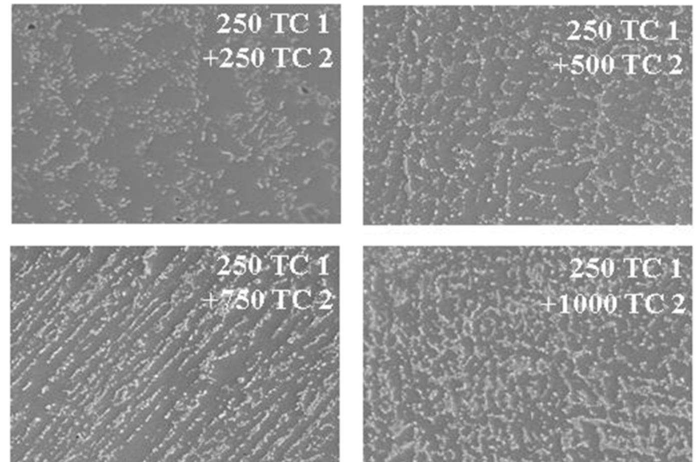

Figure 15: SEM Back-scattered Images of Phase Growth versus Multiple Environments (250 Cycles TC-1 + x-Cycles TC-2, SAC305 solder, 256 CABGA, Magnification 750x).

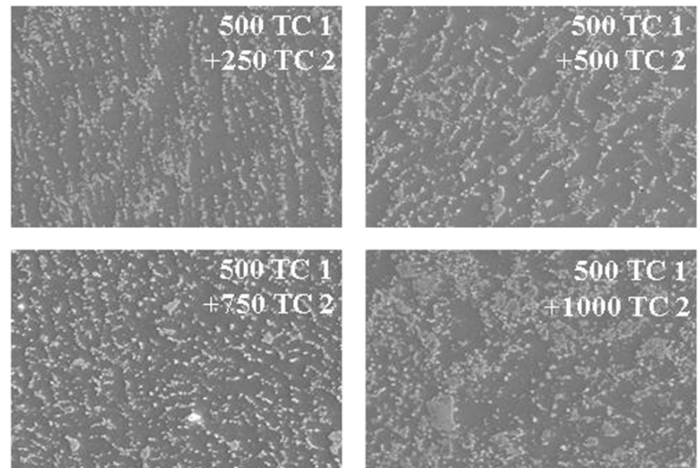

Figure 16: SEM Back-scattered Images of Phase Growth versus Multiple Environments (500 Cycles TC-1 + x-Cycles TC-2, SAC305 solder, 256 PBGA, Magnification 750x).

Three sets of assemblies have been exposed to three different sequences of multiple cyclic thermo-mechanical environments including 250 cycles of TC-1 followed by x-cycles of TC-2 (Figure 15), 500 cycles of TC-1 followed by x-cycles of TC-2 (Figure 16), and 750 cycles of TC-1 followed by x-cycles of TC-2 (Figure 17). The present dataset will be used for validation of the presented approach. Test assemblies have been previously exposed to a prognosticated number of cycles in TC-1 (500 cycles) and then redeployed in TC-2 for an unknown number of cycles have been prognosticated. The parts were withdrawn at an interval of 50 cycles to measure the phase growth in TC-2. The withdrawn samples have been cross-sectioned and the grain structure studied in an SEM. The samples were prognosticated using the Levenberg-Marquardt Algorithm. Figure 18 and Figure 19 show the prognosticated values of the 256 I/O PBGA for test assemblies that have been exposed to (500 cycles TC1 + 250 cycles TC2) and (750 cycles TC1 + 250 cycles TC2). Table

Table 4 shows the experimental and prognosticated values of the residual damage in environment TC2 for test assemblies exposed to multiple environments. The experimental values are based on the validation dataset, and the prognosticated values are based on the equation: $N_C - N_B = N_{CP} - \Delta D - N_{AP}$. The values show good correlation indicating the potential of the procedure for estimation of prior damage in presence of exposure to multiple thermal environments.

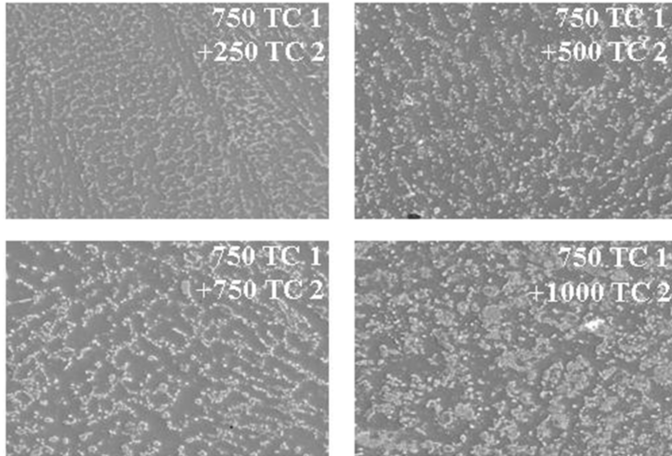

Figure 17: SEM Back-scattered Images of Phase Growth versus Multiple Environments (750 Cycles TC-1 + x-Cycles TC-2, SAC305 solder, 256 PBGA, Magnification 750x).

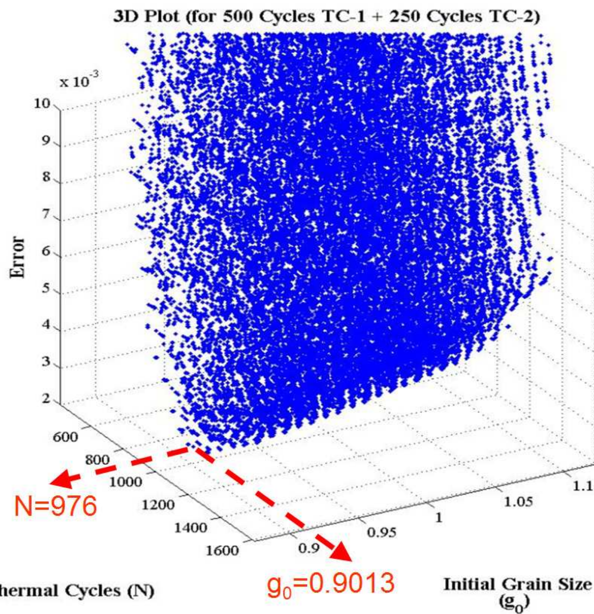

Figure 18: Prognostication for assemblies subjected to Multiple Environments. 500 Cycles TC-1 + 250 Cycles TC-2, SAC305 solder, 256 PBGA, Magnification 750x.

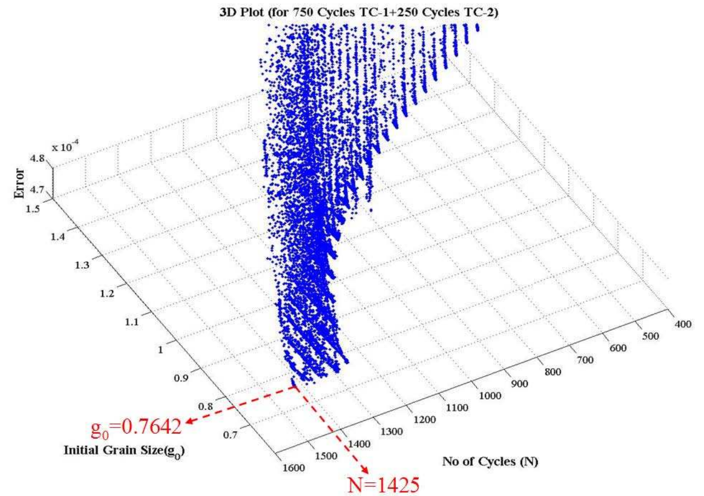

Figure 19: Prognostication for assemblies subjected to Multiple Environments. 750 Cycles TC-1 + 250 Cycles TC-2, SAC305 solder, 256 PBGA, Magnification 750x.

	Cycle Count	N_{Cp}	ΔD_p (N_{Bp} - N_{Ap})	N_{Ap}	Experiment N_C-N_B	Prognostication N_{Cp}-N_{Bp} = N_{Cp}-ΔD_p-N_{Ap}
256 I/O BGA	500 TC1 + 250 TC2	976	175	430	250	371
256 I/O BGA	750 TC1 + 250 TC2	1425	495	710	250	220

Table 4: Comparison of experimental and prognosticated values of differential damage for the 100 I/O CABGA, and 256 I/O PBGA with SAC305 interconnects.

RESIDUAL LIFE IN MULTIPLE ENVIRONMENTS

The residual life of the assemblies subjected to multiple thermal environments has been be computed based on the following equation,

$$RUL = N_{1\%} - N \tag{18}$$

Where, N1% is the time to one-percent failure of the population, N is the prognosticated prior damage in the test assemblies. The N1% may be procured by accelerated testing of the part and correlation with the field conditions. In the present case, the test assemblies were subjected to TC-1 and TC-2. The N1% value for 100CABGA packages subjected to TC-2 (0ºC to 100ºC) was calculated to be 4866 cycles (Figure 20). The RUL can be calculated as RUL = [N1% - NBp] where NBp is the prognosticated life for point-B. NBp was prognosticated to be 695 cycles respectively. Thus the residual life is RL = [4866 – 695] = 4171 cycles.

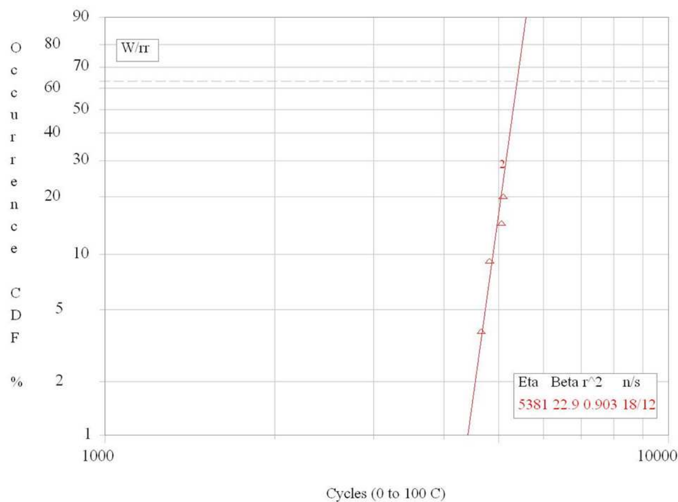

Figure 20: Weibull plot for 100CABGA packages subjected to thermal cycle 0°C to 100°C.

SUMMARY AND CONCLUSIONS

A methodology has been presented to prognosticate the accrued prior damage and assess residual life in electronics subjected to multiple thermal environments. The presented approach uses the Levenberg-Marquardt Algorithm in conjunction with microstructural evolution of damage based leading indicator for estimating prior stress history. The viability of the approach has been demonstrated for test assemblies withdrawn from one thermo-mechanical environment TC1 (-55 to 125C) and redeployed in second thermo-mechanical environment TC2 (0 to 100C). The prognostication has been demonstrated at three stages of the life cycle including, prognostication of prior stress history after withdrawal from the first environment TC1, assessment of operational readiness for redeployment in environment TC2, and the assessment of prior damage and residual life after finite time of deployment of in TC2. Model predictions of total consumed life in multiple environments correlate well with the experimental data. The correlation demonstrates that the presented leading indicator based PHM technique can be used to interrogate the system state in multiple environments and thus estimate the residual life of a component. The presented approach of computing residual life can be implemented prior to appearance of any macro-indicators of damage like crack. Methodology presented using condition monitoring components to find out the residual life is promising because these components experience the same environment as actual component.

ACKNOWLEDGEMENTS

The research presented in this paper has been supported by NASA-IVHM Program Grant NNA08BA21C from the National Aeronautics and Space Administration.

REFERENCES

Allen, D., Probabilities Associated with a Built-in-Test System, Focus on False Alarms, Proceedings of AUTOTESTCON, IEEE Systems Readiness Technology Conference, pp. 643-645, September 22-25, 2003.

Allen, S., L., Notis, Mr., R., Chromik, R., R., Vinci, R., P., Lewis, D., J., Schaefer, R., Microstructural Evolution in Lead-free Solder Alloys: Part II. Directionally solidified Sn-Ag-Cu, Sn-Cu, Sn-Ag, Journal of Materials Research, Vol. 19, No. 5, pp. 1425, May 2004b.

Allen, S., L., Notis, Mr., R., Chromik, R., R., Vinci, R.,P., Microstructural Evolution in Lead-free Solder Alloys: Part I. Cast Sn–Ag–Cu eutectic, Journal of Materials Research, Vol. 19, No. 5, pp. 1417–1424, May 2004a.

Anderson, N., and Wilcoxon, R., Framework for Prognostics of Electronic Systems, Proceedings of International Military and Aerospace Avionics COTS Conference, Seattle, WA, Aug 3-5, 2004.

Bangs, E. R., and Beal, R. E., Wel. J. Res. Supp., 54, p. 377, 1978.

Callister, Jr., W., Materials Science and Engineering: An Introduction, Wiley, New York, 1985.

Chandramouli, R., Pateras, S., Testing Systems on a Chip, IEEE Spectrum, Vol. 33, No. 11, pp. 42-47, Nov. 1996.

Drees, R., and Young, N., Role of BIT in Support System Maintenance and Availability, IEEE A&E Systems Magazine, pp. 3-7, August 2004.

Dutta, I., A Constitutive Model for Creep of Lead-Free Solders Undergoing Strain-Enhanced Microstructural Coarsening: A First Report, Journal of Electronic Materials, Vol 32, No. 4, pp. 201-207, 2003a.

Dutta, I., Impression Creep Testing and Microstructurally Adaptive Creep Modeling of Lead Free Solder Interconnects, TRC, October 25-27, 2004.

Dutta, I., Park, C., and Choi, S., Creep and Microstructural Evolution in Lead-Free Microelectronic Solder Joints, Proceedings of InterPACK '03, Paper Number IPACK2003-35209, pp.1-6, Maui, HI, July 6-11, 2003b.

Frear, D. R., Microstructural Evolution During Thermomechanical Fatigue of 62Sn-36Pb-2Ag, and 60Sn-40Pb Solder Joints, IEEE Transactions on Components Hybrids and Manufacturing Technology, Vol 13. No 4, pp. 718-726, December 1990.

Gao, R. X., Suryavanshi, A., BIT for Intelligent System Design and Condition Monitoring, IEEE Transactions on Instrumentation and Measurement, Vol. 51, Issue: 5, pp. 1061-1067, October 2002.

Hassan, A., Agarwal, V. K., Nadeau-Dostie, B., Rajski, J., BIST of PCB Interconnects Using Boundary- Scan Architecture, IEEE Transactions on Computer-Aided Design, Vol. 11, No. 10, pp. 1278-1288, October 1992.

Henderson, D., W., King, E. K., Korhonen T., M., Korhonen M., A., Lehman L., P., Cotts E., J., Kang, S., K., Lauro, P., Shih, D., Y., Goldsmith, C., Puttlitz, K., J., The Microstructure of Sn in near eutectic Sn–Ag–Cu alloy Solder Joints and its role in Thermomechanical Fatigue, Journal of Materials Research, Vol. 19, No. 6, pp. 1608–1612, June 2004.

Jarrell, D., Sisk, D., Bond, L., Prognostics and Condition Based Maintenance (CBM) A Scientific Crystal Ball, Pacific Northwest

National Laboratory, Richland, WA, International Congress on Advanced Nuclear Power Plants (ICAPP), paper number 194 June 2002.

Jung, K., Conrad, H., Microstructure Coarsening During Static Annealing of 60Sn40Pb Solder Joints: I Stereology, Journal of Electronic Materials, Oct 2001.

Kang, S., K., Lauro, P., Shih, D., Y., Henderson, D., W., Gosselin, T., Bartelo, J., Cain, S., R., Goldsmith, C., Puttlitz, K., J., Hwang, T., K., Evaluation of Thermal Fatugue and Failure Mechanisms of Sn–Ag–Cu Solder Joints with Reduced Ag Contents, 2004 Electronic Components and Technology Conference, pp. 661 – 667, 2004.

Kang, S., K., Lauro, P., Shih, D., Y., Henderson, D., W., Puttlitz, K., J., Microstructure and Mechanical Properties of Lead-free Solders and Solder Joints used in Microelectronic Applications, IBM Journal of Research and Development, Vol. 49, No. 4/5, pp. 607 – 619, July / September 2005.

Korhonen T., M., Lehman L., P., Korhonen M., A., Henderson, D., W., Isothermal Fatigue Behavior of the Near-Eutectic Sn-Ag-Cu Alloy between -25ºC and 125ºC, Journal of Electronic Materials, Vol. 36, No. 2, pp. 173 – 178, 2007.

Lall, P., Islam, N., Rahim, K., Suhling, J., Gale, S., Leading Indicators-of-Failure for Prognosis of Electronic and MEMS Packaging, 54th Electronics Components and Technology Conference, Las Vegas, Nevada, June 1 – 4, 2004a.

Lall, P., Islam, N., Shete, T., Evans, J., Suhling, J., Gale, S., Damage Mechanics of Electronics on Metal-Backed Substrates in Harsh Environments, 54th Electronic Components and Technology Conference, Las Vegas, Nevada, June 1 - 4, 2004b.

Lall, P., N. Islam, J. C. Suhling, and R. Darveaux, Model for BGA and CSP Reliability in Automotive Underhood Applications, IEEE Transactions on Components and Packaging Technologies, Volume 27, Number 3, pp. 585-593, 2004c.

Lall, P., D. Panchagade, Y. Liu, R. W. Johnson, and J. C. Suhling, Models for Reliability Prediction of Fine-Pitch BGAs and CSPs in Shock and Drop-Impact, Proceedings of the 54th Electronic Components and Technology Conference, pp. 1296-1303, Las Vegas, NV, June 1-4, 2004d.

Lall, P., Islam, N., Choudhary, P., Suhling, J., Prognostication and Health Monitoring of Leaded and Lead Free Electronic and MEMS Packages in Harsh Environments, Proceedings of the 55th IEEE Electronic Components and Technology Conference, pp. 1-9, Orlando, FL, June 1-3, 2005a.

Lall, P., Panchagade, D., Choudhary, P., Suhling, J., Gupte, S., Failure-Envelope Approach to Modeling Shock and Vibration Survivability of Electronic and MEMS Packaging, Proceedings of the 55th IEEE Electronic Components and Technology Conference, Orlando, FL, pp. 480 – 490, June 1 – 3, 2005b.

Lall, P., Gupte, S., Choudhary, P., Suhling, J., Solder-Joint Reliability in Electronics Under Shock and Vibration using Explicit Finite Element Sub-modeling, Proceedings of the 56th IEEE Electronic Components and Technology Conference, San Diego, California, pp.428-435, May 30-June 2, 2006a.

Lall, P., Choudhary, P., Gupte, S., Suhling, J., Health Monitoring for Damage Initiation & Progression during Mechanical Shock in Electronic Assemblies, Proceedings of the 56th IEEE Electronic Components and Technology Conference, San Diego, California, pp.85-94, May 30-June 2, 2006b.

Lall, P., Hande, M., Singh, N., Suhling, J., Lee, J., Feature Extraction and Damage Data for Prognostication of Leaded and Leadfree Electronics, Proceedings of the 56th IEEE Electronic Components and Technology Conference, San Diego, California, pp.718-727, May 30-June 2, 2006c.

Lall, P., Islam, N., Rahim, K., Suhling, J., Gale, S., Prognostics and Health Management of Electronic Packaging, IEEE Transactions on Components and Packaging Technologies, Volume 29, Number 3, pp. 666-677, September 2006d.

Lall, P., Islam, N., Shete, T., Evans, J., Suhling, J., Gale, S., Damage Mechanics of Electronics on Metal-Backed Substrates in Harsh Environments, IEEE Transactions on Components and Packaging Technologies, Volume 29, Number 1, pp. 204-212, March 2006e.

Lall, P., D. Panchagade, Y. Liu, R. W. Johnson, and J. C. Suhling, Models for Reliability Prediction of Fine-Pitch BGAs and CSPs in Shock and Drop-Impact, IEEE Transactions on Components and Packaging Technologies, Volume 29, Number 3, pp. 464-474, September 2006f.

Lall, P., Choudhary, P., Gupte, S., Suhling, J., Hofmeister, J., Statistical Pattern Recognition and Built-In Reliability Test for Feature Extraction and Health Monitoring of Electronics under Shock Loads, 57th Electronics Components and Technology Conference, Reno, Nevada, pp. 1161-1178, May 30-June 1, 2007a.

Lall, P., Gupte, S., Choudhary, P., Suhling, J., Solder-Joint Reliability in Electronics Under Shock and Vibration using Explicit Finite Element Sub-modeling, IEEE Transactions on Electronic Packaging Manufacturing, Volume 30, No. 1, pp. 74-83, January 2007b.

Lall, P., M. Hande, C. Bhat, J. Suhling, Jay Lee, Prognostics Health Monitoring (PHM) for Prior-Damage Assessment in Electronics Equipment under Thermo-Mechanical Loads, Electronic Components and Technology Conference, Reno, Nevada, pp. 1097-1111, May 29 – June 1, 2007c.

Lall, P. Panchagade, D., Liu, Y., Johnson, W., Suhling, J., Smeared Property Models for Shock-Impact Reliability of Area-Array Packages, ASME Journal of Electronic Packaging, Volume 129, pp. 373-381, December 2007d.

Lall, P., Hande, M., Bhat, C., Islam, N., Suhling, J., Lee, J., Feature Extraction and Damage-Precursors for Prognostication of Lead-Free Electronics, Microelectronics Reliability, Volume 47, pp. 1907–1920, December 2007e.

Lall, P., Choudhary, P., Gupte, S., Suhling, J., Health Monitoring for Damage Initiation and Progression during Mechanical Shock in Electronic Assemblies, IEEE Transactions on Components and Packaging Technologies, Vol. 31, No. 1, pp. 173-183, March 2008a.

Lall, P., Panchagade, D., Choudhary, P., Gupte, S., Suhling, J., Failure-Envelope Approach to Modeling Shock and Vibration Survivability of Electronic and MEMS Packaging, IEEE Transactions

on Components and Packaging Technologies, Vol. 31, No. 1, pp. 104-113, March 2008b.

Lall, P., Hande, M., Bhat, C., More, V., Vaidya, R., Suhling, J., Algorithms for Prognostication of Prior Damage and Residual Life in Lead-Free Electronics Subjected to Thermo-Mechanical Loads, Proceedings of the 10th Intersociety Thermal and Thermo-mechanical Phenomena (ITherm), Orlando, Florida, pp. 638-651, May 28-31, 2008c.

Lall, P., Bhat, C., Hande, M., More, V., Vaidya, R, Pandher, R., Suhling, J., Goebel, K., Interrogation of System State for Damage Assessment in Lead-free Electronics Subjected to Thermo-Mechanical Loads, Proceedings of the 58th Electronic Components and Technology Conference (ECTC), Orlando, Florida, pp. 918-929, May 27-30, 2008d.

Lall, P., Iyengar, D., Shantaram, S., S., Gupta, P., Panchagade, D., Suhling, J., KEYNOTE PRESENTATION: Feature Extraction and Health Monitoring using Image Correlation for Survivability of Leadfree Packaging under Shock and Vibration, Proceedings of the 9th International Conference on Thermal, Mechanical, and Multi-Physics Simulation and Experiments in Micro-Electronics and Micro-Systems (EuroSIME), Freiburg, Germany, pp. 594-608, April 16-18, 2008e.

Lall, P., Iyengar, D., Shantaram, S., Pandher, R., Panchagade, D., Suhling, J., Design Envelopes and Optical Feature Extraction Techniques for Survivability of SnAg Leadfree Packaging Architectures under Shock and Vibration, Proceedings of the 58th Electronic Components and Technology Conference (ECTC), Orlando, Florida, pp. 1036-1047, May 27-30, 2008f.

Lourakis, M., I., A., A brief Description of the Levenberg-Marquardt algorithm implemented by Levmar, Foundation of Research and Technology – Hellas (Forth), Greece, pp. 1- 6, Feb 11, 2005.

Madsen, K., Nielsen, H., B., Tingleff, O., Methods for Non-Linear Least Squares Problems, Technical University of Denmark, Lecture notes, available at http://www.imm.dtu.dk/courses/02611/nllsq.pdf, 2nd Edition, pp. 1-30, 2004.

Marko, K.A., J.V. James, T.M. Feldkamp, C.V. Puskorius, J.A. Feldkamp, and D. Roller, Applications of Neural Networks to the Construction of "Virtual" Sensors and Model-Based Diagnostics, Proceedings of ISATA 29th International Symposium on Automotive Technology and Automation, pp.133-138, June 3-6, 1996.

McCann, R. S., L. Spirkovska, Human Factors of Integrated Systems Health Management on Next-Generation Spacecraft, First International Forum on Integrated System Health Engineering and Management in Aerospace, Napa, CA, pp. 1-18, November 7-10, 2005.

Morris, Jr., J. W., Tribula, D., Summers, T. S. E., and Grivas D., The role of Microstructure in Thermal Fatigue of Pb/Sn Solder Joints, in Solder Joint Reliability, edited by J. H. Lau, Von Nostrand Reinhold, New York, pp. 225- 265, 1991.

Nielsen, H., B, Damping Parameter in Marquardt's Method, Technical Report, IMM-REP-1999-05, Technical University of Denmark, Available at http://www.imm.dtu.dk/˜hbn, pp. 1-16, 1999.

Rosenthal, D., and Wadell, B., Predicting and Eliminating Built-in Test False Alarms, IEEE Transactions on Reliability, Vol. 39, No 4, pp. 500-505, October 1990.

Sayama, T., Takayanagi, T. and Mori, T., Analysis of Grain Growth Process in Sn/Pb Eutectic Solder Joint, EEP-Vol. 26-1, Advances in Electronic Packaging-1999, Volume 1, ASME, 1999.

Sayama, T., Takayanagi, T., Nagai, Y., Mori, T., and Yu, Q., Evaluation of Microstructural Evolution and Thermal Fatigue Crack Initiation in Sn-Ag-Cu Solder Joints, ASME InterPACK, Paper Number IPACK2003-35096, pp.1-8, 2003.

Schauz, J. R., Wavelet Neural Networks for EEG Modeling and Classification, PhD Thesis, Georgia Institute of Technology, 1996.

Shiroishi, J., Y. Li, S. Liang, T. Kurfess, and S. Danyluk, Bearing Condition Diagnostics via Vibration and Acoustic Emission Measurements, Mechanical Systems and Signal Processing, Vol.11, No.5, pp.693-705, Sept. 1997.

Stromswold, E. I.: Characterization of eutectic tin-silver solders joints. Dissertation, University of Rochester, 1993

Tribula, D.G., Grivas, D., Frear, D., and Morris, J., Journal of Electronic Packaging, 111, pp. 83-89, 1989.

Williams, T. W., Parker, K. P., Design for Testability- Survey, Proceedings of the IEEE, Vol. 71, No. 1, pp. 98-112, January 1983.

Wolverton, A., Brazing and Soldering, 13, pp. 33, 1987.

Xiao, Q., Bailer, H., J., Armstrong, W., D., Aging Effects on Microstructure and Tensile Property of Sn3.9Ag0.6cu Solder Alloy, Transactions of the ASME, Vol. 126, pp. 208 – 212, June 2004.

Ye, L., L., Lai, Z., Liu, J., Tholen, A., Microstructural Coarsening of Lead Free Solder Joints during Thermal Cycling, Proceedings of the Electronic Components and Technology Conference, pp. 134 – 137, 2000.

Zorian, Y., A Structured Testability Approach for Multi Chip Boards Based on BIST and Boundary Scan, IEEE Transactions on Components, Packaging, and Manufacturing Technology-Part B, Vol. 17, No. 3, pp. 283-290, August 1994.

BIOGRAPHIES

Pradeep Lall is the Thomas Walter Professor in the Department of Mechanical Engineering with a joint appointment in Department of Finance. He is the Director of NSF Center for Advanced Vehicle and Extreme Environment Electronics ($CAVE^3$) at Auburn University. Dr. Lall has ten years of industry experience. He was previously with Motorola's Wireless Technology Center. He is author and co-author of 2-books, 11 book chapters, and over 225 journal and conference papers in the field of electronic packaging with emphasis on design, modeling and predictive techniques.

He is a Fellow of the ASME. Dr. Lall is a Six-Sigma Black-Belt in Statistics. Dr. Lall holds several-patents and engineering awards. Dr. Lall is an Associate Editor for the ASME Journal of Electronic Packaging, IEEE Transactions on Components and Packaging Technologies, and IEEE Transactions on Electronics Packaging Manufacturing. Dr. Lall is a member of the Beta Gamma Sigma

honorary Society. He is recipient of the Samuel Ginn College of Engineering Senior Faculty Research Award, three-Motorola Outstanding Innovation Awards, five-Motorola Engineering Awards and four-Publication Awards. He received the M.S. and Ph.D. degrees in Mechanical Engineering from University of Maryland at College Park and the M.B.A. degree from Kellogg School of Management at Northwestern University.

Rahul Vaidya received the B.E. degree in Electronics Engineering from University of Mumbai in 2006. He is currently pursuing the M.S. degree at Auburn University. He is a graduate research assistant in NSF Center for Advanced Vehicle and Extreme Environment Electronics (CAVE^3), Department of Mechanical Engineering under the guidance of Professor Pradeep Lall. His research focuses on Prognostication of lead-free electronics subjected to thermo-mechanical loading.

Vikrant More received the B.E. degree in Mechanical Engineering from University of Mumbai in 2006. He is currently pursuing the M.S. degree at Auburn University. He is a graduate research assistant in NSF Center for Advanced Vehicle and Extreme Environment Electronics (CAVE^3), Department of Mechanical Engineering under the guidance of Professor Pradeep Lall. His research areas include Prognostics of Electronic Assemblies in cyclic thermo-mechanical environments.

Kai Goebel received the degree of Diplom-Ingenieur from the Technische Universität München, Germany in 1990. He received the M.S. and Ph.D. from the University of California at Berkeley in 1993 and 1996, respectively. Dr. Goebel is a senior scientist at NASA Ames Research Center where he leads the Diagnostics & Prognostics groups in the Intelligent Systems Division. In addition, he directs the Prognostics Center of Excellence and he is the Associate Principal Investigator for Prognostics of NASA's Integrated Vehicle Health Management Program. He worked at General Electric's Corporate Research Center in Niskayuna, NY from 1997 to 2006 as a senior research scientist. He has carried out applied research in the areas of artificial intelligence, soft computing, and information fusion. His research interest lies in advancing these techniques for real time monitoring, diagnostics, and prognostics. He holds eleven patents and has published more than 150 papers in the area of systems health management.